View Article Online / Journal Homepage / Table of Contents for this issue

# The change in the electronic character upon cisplatin binding to guanine nucleotide is transmitted to drive the conformation of the local sugar-phosphate backbone—a quantitative study

**Matjaž Polak,[a] Janez Plavec,*[a] Anna Trifonova,[b] Andras Földesi[b] and Jyoti Chattopadhyaya *[b]**

[a] *National Institute of Chemistry, Hajdrihova 19, SI-1115 Ljubljana, Slovenia. E-mail: janez.plavec@ki.si*
[b] *Department of Bioorganic Chemistry, Box 581, Biomedical Centre, University of Uppsala, S–751 23 Uppsala, Sweden. E-mail: jyoti@bioorgchem.uu.se*

***Received (in Cambridge, UK) 23rd March 1999, Accepted 6th August 1999***

Published on 01 January 1999. Downloaded on 22/10/2014 10:06:02.

The microstructure alteration as a result of cisplatin binding to N7 of guanines in DNA has been herein assessed through the multinuclear temperature-, pH*- and concentration-dependent NMR study of the effect of $Pt^{2+}$ complexation to 2′-deoxyguanosine 3′,5′-bis(ethyl hydrogen phosphate) **1** and its *ribo* analogue **3** which mimic the central nucleotide moiety in a trinucleoside diphosphate in the complete absence of intramolecular base–base stacking interactions. The $N \rightleftharpoons S$ pseudorotational equilibrium shifts towards *N*-type conformers by 17 and 21 percentage points at 298 K, respectively, thereby showing that free energy of platination is transmitted to drive the sugar conformation. The increase in the population of *N*-type conformers was rationalized with the strengthening of the anomeric effect in both 2′-deoxy and *ribo* nucleotides upon the formation of the Pt–N7 bond which promotes $n_{O4'} \rightarrow \sigma^*_{C1'\text{-}N9}$ orbital interactions due to the reduction of π-electron density in the imidazole part of guanine. The additional stabilization of *N*-type conformers in $Pt^{2+}$ complexes of ribonucleotides is due to the tuning of the *gauche* effect of the [N9–C1′–C2′–O2′] fragment, which is absent in 2′–deoxy-*ribo* counterparts. The platination of N7 favours N1 deprotonation in **2** and **4** by $\Delta pK_a$ of 0.7 and 0.9 units in comparison with parent nucleotides **1** and **3**, respectively. The $N \rightleftharpoons S$ pseudorotational equilibrium in **1**–**4** showed classical sigmoidal dependence as a function of pH with $pK_a$-values at the inflection points. The population of *S*-type conformers has increased upon N1 deprotonation in **1**–**4** because the anomeric effect weakened due to the increased π-electron density in the imidazole part of the guanine moiety. The formation of the Pt–N7 bond in bifunctional complexes **2** and **4** simultaneously causes a shift of the *syn* $\rightleftharpoons$ *anti* equilibrium towards *anti* by 43 and 63 percentage points, and the increase in the population of $\varepsilon^{t,N}$ conformers by 20 and 32 percentage points at 278 K, respectively. Only a minor conformational redistribution along $\beta$, $\gamma$, $\beta^{+1}$ and $\varepsilon^{-1}$ torsion angles has been observed, which suggests their weak conformational cooperativity with the $N \rightleftharpoons S$ pseudorotational equilibrium as a result of platination to guanine. In comparison with nucleotide phosphodiesters, apurinic 3′,5′-bis(ethyl hydrogen phosphate) sugars **5** and **6** showed no interaction with $Pt^{2+}$ and therefore no conformational changes.

## Introduction

The anticancer drug cisplatin manifests its therapeutic activity by reacting with DNA to form crosslinks as major lesions, thus interfering with replication and transcription processes.[1] Various studies have shown that platinum is coordinated by the N7 of guanines and adenines which agrees, with its 'soft' metal ion nature and thus has greater affinity for nitrogen donors than 'hard' oxygen ligands of phosphodiester functionalities.[2–11] It is well known from numerous X-ray studies[12–14] that sugar moieties in natural nucleosides adopt predominantly two distinct North (*N*, roughly C3′-*endo*) and South (*S*, roughly C2′-*endo*) conformational families (Fig. 1). NMR studies in solution have shown that the sugar moieties of nucleosides and nucleotides are involved in a two-state conformational equilibrium between *N* and *S* puckered forms which are dynamically interconverting on the NMR time-scale. We have previously quantified the thermodynamics of $N \rightleftharpoons S$ pseudorotational equilibrium and shown that it is driven by the interplay of stereoelectronic anomeric and *gauche* effects as well as by the competing steric effects of the substituents.[15,16] The *gauche* effects of C3′–O3′ and C2′–O2′ bonds with C4′–O4′ and C1′–O4′ bonds drive the $N \rightleftharpoons S$ equilibrium towards *S*- and *N*-type conformers, respectively. The nucleobase in *N*-nucleosides influences the drive of the $N \rightleftharpoons S$ equilibrium through inherent steric effects and the O4′–C1′–N1/9 anomeric effect. It has been shown that the anomeric effect of guanine is strengthened by N7 protonation[17] or by interaction with 'soft' $M^{2+}$ ions.[18,19] A conformational rearrangement has been observed in DNA–cisplatin adducts[20] which can clearly be ascribed to the binding of $Pt^{2+}$ to N7 of guanine. Little is, however, known of how the $Pt^{2+}$ binding to N7 of guanine nucleobase changes its stereoelectronic properties and how these are transmitted into the drive of the local sugar-phosphate backbone conformation. In the present study we have synthesized 2′-deoxyguanosine 3′,5′-bis(ethyl hydrogen phosphate) **1** and its *ribo* analogue **3**, which serve as model systems mimicking the central nucleotide moiety in a trinucleoside diphosphate in order to shed light on the nature and strength of intramolecular stereoelectronic effects in the complete absence of intramolecular base–base stacking interactions (Chart 1). The temperature- and pH-dependent conformational analysis on apurinic sugars **5** and **6** enabled the comparison and dissection of the conformational changes caused by the transmission of the strengthened anomeric effect in platinated nucleotides **2** and **4** from the drive of the conformational equi-



**This journal is © The Royal Society of Chemistry 1999**

View Article Online

Published on 01 January 1999. Downloaded on 22/10/2014 10:06:02.

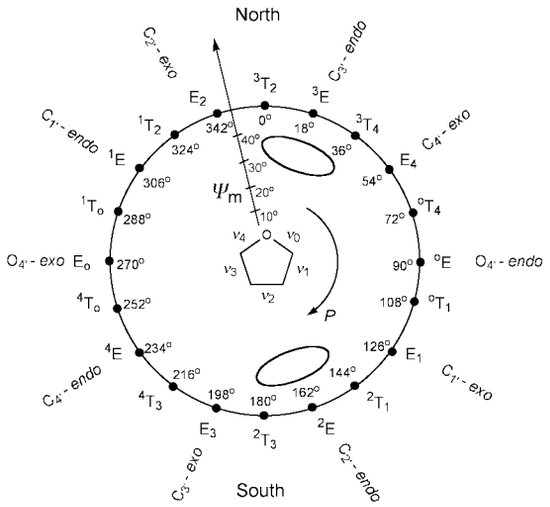


**Fig. 1** Pseudorotation cycle of the pentofuranose ring in nucleosides and nucleotides. Two pseudorotational parameters $P$ and $\Psi_m$, which have been proposed by Altona and Sundaralingam,[13] are used to describe the geometry of the puckered five-membered ring; $P$ is the phase angle of pseudorotation and $\Psi_m$ is the maximum puckering amplitude. In the pseudorotational cycle, the sugar geometries alternate between envelope ($E$) and twist ($T$) conformations every $P$ of 18°. $\Psi_m$ denotes the extent of puckering and increases with the radial displacement. The conformational regions that are most commonly found by X-ray crystallography and NMR studies in solution are shaded in the North and South regions of conformational space.

libria along sugar-phosphate torsion angles due to the possible interactions of $Pt^{2+}$ with phosphodiester moieties in **5** and **6** to be made.

## Results and discussion

### Formation and identification of reaction products between *cis*-$[Pt(ND_3)_2(D_2O)_2]^{2+}$ and 1, 3, 5 and 6

The reactions of *cis*-$[Pt(ND_3)_2(D_2O)_2]^{2+}$ with **1**, **3**, **5** and **6** in $D_2O$ were monitored by $^1H$ NMR spectroscopy. Preliminary experiments showed that the reaction of one equivalent of *cis*-$[Pt(ND_3)_2(D_2O)_2]^{2+}$ with **1** resulted in the fast formation[21,22] (<10 min at 298 K) of monoplatinated complex ($\delta_{H8} = 8.60$), which was further transformed into the bifunctional complex **2** ($\delta_{H8} = 8.50$) together with several other products. The complex reaction mixture prevented the extraction of coupling constants for the individual species. On the other hand, the complexation of **1** and **3** with 0.5 equivalents of *cis*-$[Pt(ND_3)_2(D_2O)_2]^{2+}$ resulted in one predominant set of $^1H$ NMR resonances corresponding to bisnucleotide $Pt^{2+}$ complexes **2** and **4**, respectively (Chart 1). The amount of complexes **2** and **4** in the NMR tubes was over 90%. The detailed $^1H$, $^{13}C$, $^{15}N$, $^{31}P$ and $^{195}Pt$ NMR chemical-shift analysis given in Table 1 confirmed the presence of two guanine moieties in the $Pt^{2+}$ coordination plane and therefore the structures of **2** and **4**. $^{31}P$ chemical-shift changes upon coordination of **1** and **3** with $Pt^{2+}$ are insignificant and thus clearly exclude the formation of an N7, PO chelate[23] in **2** and **4** (Table 1).

The effect of temperature on the H8 linewidths in bifunctional complexes **2** and **4** was studied to assess the rate of rotation about the Pt–N7 bonds. The H8 signals sharpen with an increase in temperature from 278 to 358 K from 2.3 to 1.0 Hz in **2** and from 3.7 to 1.1 Hz in **4**, which indicates that nucleotide moieties are in the fast Pt–N7 rotation-rate regime on the NMR time-scale at all studied temperatures. For comparison, the H8 resonances in the parent nucleotides sharpened from 2.8 to 1.1 Hz in **1** and from 5.4 to 1.4 Hz in **3** as temperature was increased from 278 to 358 K.

No chemical-shift changes were observed upon addition of *cis*-$[Pt(ND_3)_2(D_2O)_2]^{2+}$ to abasic compounds **5** and **6**, which

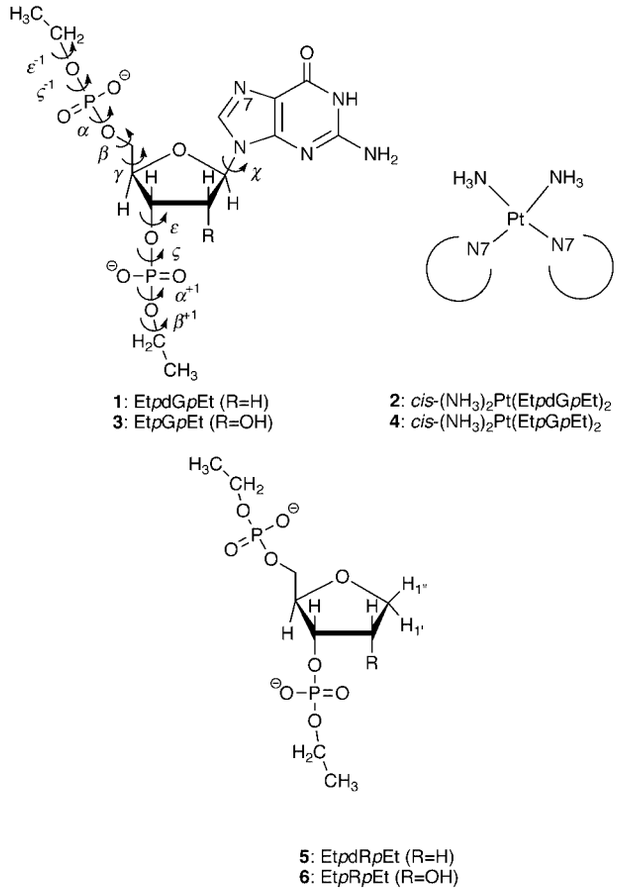


**Chart 1** Structural formulas of ligands **1**, **3**, **5** and **6** and schematical formula of bifunctional platinum complexes **2** and **4**.

gave clear evidence for the lack of their interaction with $Pt^{2+}$ in the absence of the heterocyclic nucleobase (Table 1). The $\Delta\delta(^{31}P)$-values of both 3′- and 5′-phosphodiesters in **5** and **6** are below 0.06 ppm (Table 1),[24] which indicates that electrostatic interactions of positive platinum and negative phosphate oxygen atoms are minimal.

### Self-association of nucleotides 1 and 3 and their platinated complexes 2 and 4

The $^1H$ NMR chemical shifts for **1**–**4** at eight concentrations in the range from 227 mM to 1 mM have been collected to study their self-association. The $^1H$ NMR chemical-shift changes of H8 and all sugar resonances of **1**–**4** showed only minute concentration dependence ($\Delta\delta < 0.045$ ppm). Nevertheless, the concentration-dependent chemical shifts were further analyzed according to the isodesmic EK model.[25] The analysis of small $\Delta\delta$-values of H8, H1′, H2′ and H3′ in **1**–**4** afforded small average individual association constants ($K_{av} = 1 \pm 1\ M^{-1}$) for **1**–**4** which indicated the presence of over 96% (± 3%) of monomeric species at 20 mM concentration, which value was used in the present multinuclear NMR conformational study.

### Acid–base properties of nucleotides 1 and 3 and their platinated complexes 2 and 4

Nucleotides **1** and **3** and their $Pt^{2+}$ complexes **2** and **4** may release a proton from N1. Analysis of the H8 chemical shift in **1** and **3** as a function of pH* in the range from 5.3 to 12.5 showed classical sigmoidal dependence (Fig. 2A) (For a definition of pH* see Experimental section.). The least-squares fitting procedure and Hill plots (not shown) gave p$K_a$-values of 10.2 for both **1** and **3**. The pH* dependence of H8 chemical shifts in **2** and **4** which is shown in Fig. 2A yielded p$K_a$-values of 9.5 and 9.1, respectively. The platination of N7 therefore favoured N1 deprotonation in **2** and **4** by a $\Delta pK_a$ of 0.7 and 0.9 units in

View Article Online

Published on 01 January 1999. Downloaded on 22/10/2014 10:06:02.

**Table 1** $^{1}$H, $^{13}$C, $^{31}$P, $^{15}$N, $^{195}$Pt NMR chemical shifts[a] for **1**–**6** at 298 K at neutral pH*

| Compound | **1** | **2** | **3** | **4** | **5** | **5** + **Pt**[b] | **6** | **6** + **Pt**[b] |
|---|---|---|---|---|---|---|---|---|
| H8 | 8.081 | 8.502 | 8.103 | 8.534 | | | | |
| H1′ | 6.359 | 6.311 | 5.988 | 5.959 | 3.985 | 3.986 | 3.840 | 3.842 |
| H1″ | | | | | 4.085 | 4.086 | 4.104 | 4.106 |
| H2′ | 2.930 | 2.844 | 4.945 | HOD | 2.230 | 2.232 | 4.438 | 4.440 |
| H2″ | 2.723 | 2.756 | | | 2.148 | 2.149 | | |
| H3′ | 5.014 | 5.002 | 4.836 | 4.830 | 4.690 | 4.691 | 4.522 | 4.523 |
| H4′ | 4.435 | 4.423 | 4.537 | 4.515 | 4.186 | 4.188 | 4.165 | 4.168 |
| H5′ | 4.063 | 4.093 | 4.109 | 4.176 | 3.920 | 3.921 | 4.089 | 4.091 |
| H5″ | 4.063 | 4.043 | 4.109 | 4.129 | 3.871 | 3.872 | 3.930 | 3.932 |
| 3′-C$H_2$ | 3.996 | 3.989 | 4.024 | 4.014 | 3.947 | 3.947 | 3.983 | 3.984 |
| 5′-C$H_2$ | 3.783 | 3.828 | 3.846 | 3.901 | 3.947 | 3.947 | 3.950 | 3.951 |
| 3′-C$H_3$ | 1.304 | 1.298 | 1.303 | 1.294 | 1.278 | 1.278 | 1.288 | 1.288 |
| 5′-C$H_3$ | 1.122 | 1.103 | 1.162 | 1.159 | 1.274 | 1.274 | 1.274 | 1.275 |
| C6 | 162.24 | 159.81 | 162.21 | 159.82 | | | | |
| C4 | 157.10 | 157.74 | 157.17 | 157.80 | | | | |
| C2 | 154.82 | 153.59 | 155.26 | 153.75 | | | | |
| C8 | 140.87 | 143.25 | 140.86 | 143.39 | | | | |
| C5 | 119.52 | 117.36 | 119.59 | 117.32 | | | | |
| C1′ | 88.14 | 88.43 | 89.66 | 91.26 | 66.99 | 67.00 | 74.88 | 74.90 |
| C4′ | 86.93 | 88.04 | 86.45 | 86.33 | 83.48 | 83.49 | 83.16 | 83.17 |
| C3′ | 78.98 | 78.19 | 77.39 | 76.80 | 76.55 | 76.57 | 78.18 | 78.39 |
| C2′ | 40.91 | 41.26 | 75.93 | 76.33 | 32.82 | 32.84 | 73.45 | 73.46 |
| C5′ | 68.39 | 68.24 | 68.09 | 67.84 | 64.82 | 64.85 | 68.23 | 68.25 |
| 3′-C$H_2$ | 65.73 | 65.81 | 65.86 | 65.91 | 61.93 | 61.95 | 65.55 | 65.57 |
| 5′-C$H_2$ | 65.46 | 65.52 | 65.54 | 65.58 | 61.89 | 61.91 | 65.36 | 65.38 |
| 3′-C$H_3$ | 18.89 | 18.94 | 18.90 | 18.90 | 15.20 | 15.22 | 18.66 | 18.68 |
| 5′-C$H_3$ | 18.63 | 18.68 | 18.69 | 18.71 | 15.16 | 15.18 | 18.59 | 18.61 |
| P5′ | 1.00 | 0.94 | 1.00 | 0.98 | 1.29 | 1.30 | 1.26 | 1.27 |
| P3′ | 0.36 | 0.36 | 0.57 | 0.58 | 0.53 | 0.54 | 0.72 | 0.72 |
| N7 | −145.9 | −239.1 | −145.9 | −238.1 | | | | |
| N9 | −208.2 | −203.4 | −213.5 | −209.2 | | | | |
| Pt | | −2441 | | −2442 | | −1615 | | −1615 |

[a] Chemical shifts are in ppm (±0.001 ppm for $^{1}$H, ±0.01 ppm for $^{13}$C and $^{31}$P, ±0.05 ppm for $^{15}$N and ±1 ppm for $^{195}$Pt). The methylene protons of ethyl phosphodiester groups showed $\Delta\delta$ < 16 Hz. HOD denotes that H2′ was hidden under the residual water signal. [b] **5** + **Pt** and **6** + **Pt** represent solutions of **5** and **6** in the presence of *cis*-[Pt(ND$_3$)$_2$(D$_2$O$_2$)]$^{2+}$, respectively.

comparison to parent nucleotides **1** and **3**, respectively. The increased acidity[8,11] of N1 in **2** and **4** can be explained by the reduction of electron density at N1 by the electron-withdrawing effect of the *cis*-[Pt(ND$_3$)$_2$]$^{2+}$ moiety. It is noteworthy that compounds **1**–**4** are protonated at N1 by over 99.5% at a pH* of 6.8, which was a pH* value used in our conformational studies.

### North⇌South pseudorotational equilibrium

The conformational analysis of the pentofuranosyl moiety in **1**–**6** was based on the temperature-dependent $^{3}J_{HH}$ proton–proton coupling constants (Table 2), which were interpreted in terms of a two-state $N\rightleftharpoons S$ pseudorotational equilibrium (Table 3). The experimental $^{3}J_{HH}$ coupling constants which were acquired at five temperatures in the range from 278 to 358 K were analysed with the computer program PSEUROT.[26,27] The $N\rightleftharpoons S$ pseudorotational equilibrium in both **1** and **3** is biased towards *S* by 77% at 298 K. On the other hand, their platinated complexes **2** and **4** exhibit smaller conformational purities of 60 and 56% of *S*-type sugar conformation at 298 K, respectively. There is therefore a definite drive of the $N\rightleftharpoons S$ pseudorotational equilibrium towards *N*-type sugar conformations by 17 percentage points in **2** compared with **1**, and by 21 percentage points in **4** compared with **3** at 298 K.

The mole fractions of *N*- and *S*-type conformers at five temperatures between 278 and 358 K in 20 K steps were used in a van't Hoff-type analysis to obtain enthalpy ($\Delta H°$) and entropy ($\Delta S°$) of the $N\rightleftharpoons S$ pseudorotational equilibrium in **1**–**6**. Nucleotides **1** and **3** exhibited negative $\Delta H°$-values which predominate over the weaker $-T\Delta S°$ contributions in the drive of their $N\rightleftharpoons S$ equilibrium towards *S*-type pseudorotamers (Table 3). Their platinated complexes **2** and **4** were characterized by small $\Delta H°$ values as compared with the relatively stronger $-T\Delta S°$ contributions (Table 3). The experimental $\Delta H°$-values reflect the balance of anomeric and *gauche* effects of [O4′–C4′–C3′–O3′] fragments in 2′-deoxy analogues **1** and **2**. In **2**, the platination of N7 modulates exclusively the anomeric effect which has been observed by monitoring the increase in the relative ratio of pseudoaxial (*i.e.* in *N*-type pseudorotamers) over pseudoequatorial (*i.e.* in *S*-type pseudorotamers) orientations of the nucleobase. The comparison of $\Delta H°$-values in **1** and **2** shows that the anomeric effect of guanine in **2** is strengthened by a value for $\Delta\Delta H°$ of 3.5 kJ mol$^{-1}$ which results in the drive of the $N\rightleftharpoons S$ equilibrium towards *N*-type pseudorotamers. The $N\rightleftharpoons S$ pseudorotational equilibrium of *ribo* analogues **3** and **4** is in contrast to that of 2′–deoxy counterparts **1** and **2** additionally controlled by the *gauche* effects of [O4′–C1′–C2′–O2′] fragments, which stabilize the *N*-type conformation, and by the *gauche* effects of [N9–C1′–C2′–O2′] fragments, which stabilize the *S*-type sugar conformation.[15] The data in Table 3 show that the overall drive of $N\rightleftharpoons S$ equilibrium towards *N*-type sugar conformations upon platination of *ribo* nucleotide **3** is strengthened by a value for $\Delta\Delta H°$ of 4.9 kJ mol$^{-1}$. It is therefore apparent that a platinum atom bound to N7 of guanine in **4** modulates the anomeric effect as well as the *gauche* effect of the [N9–C1′–C2′–O2′] fragment, which results in the additional stabilization of *N*-type pseudorotamers in *ribo* analogue **4** in comparison with its 2′-deoxy counterpart **2** (Table 3).

The conformational analyses of 2′-deoxy sugar **5** showed a high conformational bias of 85% towards *S*-type sugar puckering at 278 K (Table 3). The van't Hoff analysis showed that $N\rightleftharpoons S$ equilibrium in **5** is driven towards *S* by larger $\Delta H°$ values, which is opposed by the weaker entropy term. The addition of Pt$^{2+}$ reagent caused no observable tuning of the $N\rightleftharpoons S$ equilibrium in **5** (Table 3). The analysis of temperature-dependent $^{3}J_{HH}$ values in **6** before and after addition of Pt$^{2+}$ (Table 2) showed nearly identical conformational preferences of 73% for *N*-type sugar at 278 K (Table 3). The pseudorotational

View Article Online

Published on 01 January 1999. Downloaded on 22/10/2014 10:06:02.

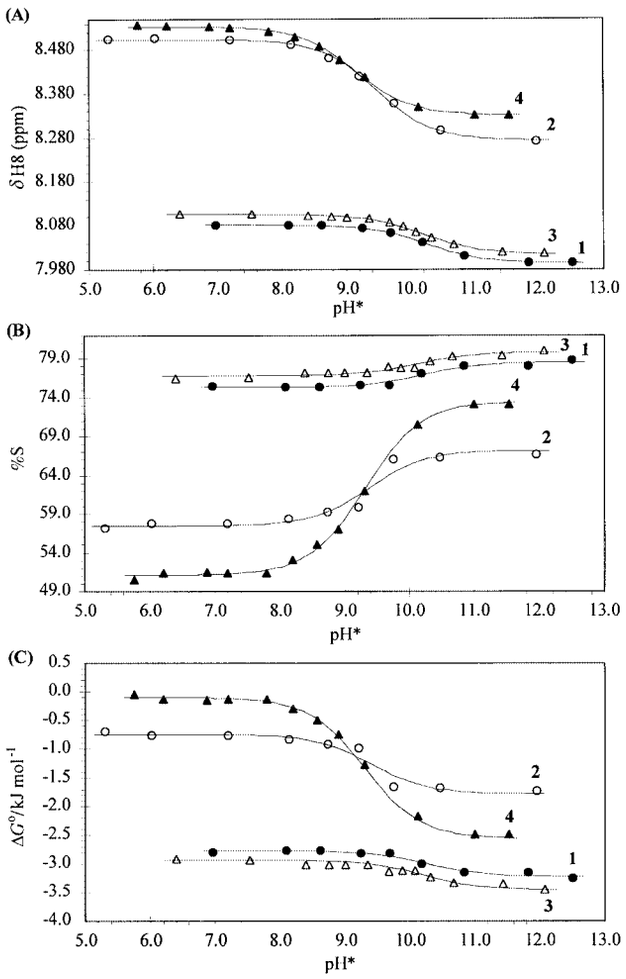


**Fig. 2** p$K_a$ Determination of **1**–**4** on the basis of pH-dependent chemical shifts of H8 (A), populations of *S*-type conformers (B) and $\Delta G°$ of $N \rightleftharpoons S$ pseudorotational equilibrium (C). Panel (A): Titration curves constructed from H8 chemical shifts as a function of pH* at 298 K in **1** (filled circles), **2** (open circles), **3** (open triangles) and **4** (filled triangles). The sigmoidal curves are the best iterative least-squares fit (r.m.s. error < 0.003 ppm) of the experimental pH*-dependent chemical shifts giving the p$K_a$-values at the inflection points. The p$K_a$-values are 10.2 for **1** and **3**, 9.5 for **2** and 9.1 for **4**. Panel (B): The population of *S*-type conformers as a function of pH* for **1**–**4** at 298 K. The sigmoidal curves which are the best iterative least-squares fit (r.m.s. error < 0.9 percentage points) of the pH*-dependent mole fractions of *S*-type conformers in the two state $N \rightleftharpoons S$ pseudorotational equilibrium are characterized by the following p$K_a$-values: 10.2 for **1** and **3**, 9.4 for **2** and 9.5 for **4**. The populations of *S*-type conformers on plateaux raised by 3.2 percentage points (from 75.5 to 78.7%) for **1**, by 9.6 percentage points (from 57.1 to 66.7%) for **2**, by 3.7 percentage points (from 76.4 to 80.1%) for **3** and by 22.6 percentage points (from 50.5 to 73.1%) for **4**. Panel (C): pH*-dependent $\Delta G°$ for the $N \rightleftharpoons S$ equilibrium in **1**–**4** at 298 K. The best fit through the experimental data points gave identical p$K_a$-values to those in panel (B). The changes in the experimental $\Delta G°$-values upon N1-deprotonation were: −0.45 kJ mol$^{-1}$ for **1**, −1.0 kJ mol$^{-1}$ for **2**, −0.5 kJ mol$^{-1}$ for **3** and −2.55 kJ mol$^{-1}$ for **4**.

equilibrium in **6** is driven towards *N*-type conformers by the $\Delta H°$ term, which is opposed by the twice weaker entropy term.

The $N \rightleftharpoons S$ pseudorotational equilibrium in **1**–**4** was also assessed as a function of pH*, which showed classical sigmoidal dependence (Fig. 2B). The population of *S*-type conformers at 298 K increased upon N1 deprotonation from 76 to 79% in **1**, from 57 to 67% in **2**, from 76 to 80% in **3** and from 51 to 73% in **4** (Fig. 2B). Our previous studies [17] have shown that the thermodynamics of N1 deprotonation in guanine nucleosides is transmitted to drive the $N \rightleftharpoons S$ equilibrium towards *S*-type pseudorotamers. The drive of $N \rightleftharpoons S$ equilibrium towards *S* can be explained by the weakening of the anomeric effect due to the increased electron density on the heterocyclic nucleobase caused by N1 deprotonation. Inspection of sigmoidal curves in Fig. 2B shows that the increase in the population of *S*-type conformers has been considerably more pronounced in bifunctional platinated complexes **2** and **4** in comparison with their parent nucleotides **1** and **3**, respectively. The $Pt^{2+}$ bound to N7 obviously promotes the re-distribution of the electronic density from anionic deprotonated N1 into the imidazole part of the guanine moieties in **2** and **4**. The increase of the electron-rich character of imidazole weakens $n_{O4'} \rightarrow \sigma^*_{C1'-N9}$ interactions which is manifested in the larger shift towards *S*-type conformers in platinum complexes **2** and **4** in comparison with their parent nucleotides. The much higher preference for *S*-type conformers in *ribo* analogue **4** in comparison with its 2′-deoxy counterpart **2** (Fig. 2B) can be explained by the additional drive of the $N \rightleftharpoons S$ equilibrium by the *gauche* effects of [O2′–C2′–C1′–N9] and [O4′–C1′–C2′–O2′] fragments. The combination of the weakened anomeric effect and the strengthened *gauche* effect of the [O2′–C2′–C1′–N9] fragment in **4** upon N1 deprotonation results in the large conformational bias of the $N \rightleftharpoons S$ pseudorotational equilibrium towards *S*-type conformers (Table 3, Fig. 2B).

Van't Hoff-type analysis of temperature-dependent populations of the *N*- and *S*-type conformers in N1 deprotonated **1**–**4** gave $\Delta H°$- and $\Delta S°$-values for the $N \rightleftharpoons S$ pseudorotational equilibrium (Table 3). Deprotonation of 2′-deoxy nucleotides **1** and **2** unexpectedly resulted in an increase in the $\Delta H°$-values of the $N \rightleftharpoons S$ equilibrium, which indicates a drive towards *N*-type conformations. However, the stronger opposing entropy term has prevailed, which results in a decrease in $\Delta G°$ for **1** and **2** (Fig. 2C) and therefore the overall stabilization of the *S*-type sugar conformation upon N1 deprotonation (Table 3). The deprotonation of ribonucleotide **3** and its $Pt^{2+}$ complex **4** results in a decrease in $\Delta H°$ by 1.4 and 7.0 kJ mol$^{-1}$, respectively (Table 3). The weaker entropy terms in **3** and **4** drive $N \rightleftharpoons S$ equilibrium towards *N*, but the overall stabilization of *S*-type sugar conformations has been observed upon N1 deprotonation for both **3** and **4** (Table 3).

### Conformational equilibrium across the C1′–N9 ($\chi$) bond

Semiquantitative information about the conformational equilibrium across glycosyl bonds in **1**–**4** has been obtained with the use of 1D NOE spectroscopy.[28] Analyses of H8→H1′ NOE enhancements have shown that the populations of *anti* conformers are 53 and 29% in **1** and **3**, respectively. Their platinated complexes **2** and **4** have shown a high conformational bias towards *anti* of 96 and 92%, respectively. The strong preference for *anti* conformers upon binding of $Pt^{2+}$ to N7 in **2** and **4** can be explained by the increased steric bulk which forces the heterocyclic moiety to turn away from the sugar moiety. The large increase in the population of *anti* conformers in **2** and **4** in comparison with **1** and **3**, respectively, is correlated with the increase in the population of *N*-type pseudorotamers. It is noteworthy that the larger shift of $N \rightleftharpoons S$ equilibrium towards *N*-type pseudorotamers upon platination of *ribo* analogue **3** in comparison with its 2′-deoxy counterpart **1** (Table 3) correlates with the larger shift of their *syn*$\rightleftharpoons$*anti* equilibrium towards *anti*.

### Conformational equilibrium across the C5′–O5′ ($\beta$) bond

The conformational equilibrium across torsion angle $\beta$[C4′–C5′–O5′–P] has been assessed with the use of temperature-dependent $^3J_{C4'P}$ and the sum of $^3J_{H5'P}$ and $^3J_{H5''P}$ coupling constants [29–31] (Table 2). The analysis of both sets of coupling constants gave comparable results with discrepancies below 3 percentage points, which is well within the accuracy of the Karplus equations used. The average populations of $\beta^t$ rotamers at the two limiting temperatures are reported in Table 4. $\beta^t$ conformers are preferred by over 75% in **1**–**6** at 278 K. This value is lowered by ≈4 percentage points when the temperature

View Article Online

Published on 01 January 1999. Downloaded on 22/10/2014 10:06:02.

**Table 2** $J_{HH}$, $J_{HP}$ and $J_{CP}$ coupling constants for **1**–**6** at two limiting temperatures at neutral pH*[a]

| Comp. | $T$(K) | $J_{HH}$ | | | | | | | | $J_{HP}$ | | | $J_{CP}$ | | |
|---|---|---|---|---|---|---|---|---|---|---|---|---|---|---|---|
| | | 1′2′ | 1′2″ | 1″2′ | 1″2″ | 2′3′ | 2″3′ | 3′4′ | 4′5′ | 4′5″ | H3′P3′ | H5′P5′ | H5″P′ | C2′P3′ | C4′P3′ | C4′P5′ |
| **1** | 278 | 8.1 | 6.2 | | | 5.8 | 2.5 | 2.2 | 4.3 | 3.0 | 7.1[a] | 4.2 | 4.5 | 3.6 | 6.0 | 9.0 |
| | 358 | 7.8 | 6.3 | | | 6.1 | 2.9 | 2.7 | 3.4 | 5.1 | 7.5 | 4.9 | 5.0 | 3.2 | 6.3 | 8.7 |
| **2** | 278 | 6.2 | 6.7 | | | 6.3 | 4.1 | 3.3 | 3.2 | 4.4 | 7.2[a] | 4.5 | 4.5 | 2.4 | 6.6 | 8.2 |
| | 358[b] | 6.5 | 6.6 | | | 6.1 | 4.1 | 3.3 | 3.5 | 5.0 | 7.1 | 5.1 | 5.1 | 3.0 | 6.1 | 7.9 |
| **3** | 278 | 6.9 | | | | 5.2 | | 2.5 | 2.7 | 3.5 | 7.8 | 4.6 | 3.9 | 4.9 | 2.9 | 9.0 |
| | 358 | 6.4 | | | | 5.2 | | 3.2 | 2.8 | 4.5 | 7.5 | 4.9 | 4.9 | 4.0 | 4.3 | 8.5 |
| **4** | 278 | 5.0 | | | | 4.9 | | 4.3 | 2.4 | 3.8 | 7.8 | 5.1 | 4.6 | 3.4 | 6.2 | 8.7 |
| | 358[b] | 5.1 | | | | 5.1 | | 4.3 | 2.8 | 4.8 | 7.7 | 5.2 | 4.8 | 3.7 | 5.8 | 8.7 |
| **5** | 278 | 10.0 | 6.2 | 8.3 | 2.8 | 5.8 | 2.1 | 1.7 | 3.7 | 5.4 | 7.3 | 4.9 | 5.2 | 3.2 | 6.5 | 8.4 |
| | 358 | 9.3 | 6.6 | 8.2 | 3.7 | 6.0 | 2.4 | 2.4 | 3.9 | 5.7 | 7.0 | 5.3 | 5.7 | 3.3 | 6.3 | 8.1 |
| **5** + **Pt** | 278 | 10.0 | 6.2 | 8.3 | 2.9 | 5.7 | 2.0 | 1.9 | 3.8 | 5.3 | 7.2 | 4.9 | 5.1 | 3.5 | 6.3 | 8.4 |
| | 358[b] | 9.3 | 6.6 | 8.2 | 3.7 | 6.0 | 2.4 | 2.4 | 4.0 | 5.7 | 7.0 | 5.4 | 5.7 | 3.3 | 6.3 | 8.2 |
| **6** | 278 | 3.2 | | 4.3 | | 4.6 | | 6.3 | 2.4 | 5.0 | 8.1 | 5.2 | 4.7 | 3.3 | 6.6 | 8.7 |
| | 358 | 3.8 | | 4.9 | | 4.9 | | 6.0 | 2.7 | 5.5 | 7.5 | 5.4 | 5.5 | 3.3 | 6.3 | 8.5 |
| **6** + **Pt** | 278 | 3.2 | | 4.3 | | 4.7 | | 6.4 | 2.4 | 5.1 | 8.1 | 5.1 | 4.7 | 3.4 | 6.3 | 8.5 |
| | 358[b] | 3.8 | | 4.7 | | 5.0 | | 5.9 | 2.8 | 5.6 | 7.5 | 5.4 | 5.3 | 3.4 | 6.3 | 8.1 |

[a] Homo- and hetero-nuclear coupling constants are given in Hz (±0.1 Hz for $^3J_{HH}$ and $^3J_{HP}$, ±0.2 Hz for $^3J_{CP}$). H3′ signals were hidden under HOD signal and $^3J_{H3'P3'}$ coupling constants at 278 K were extrapolated according to the trend with temperature. [b] The highest temperature for the collection of $^{13}C$ NMR data for complexes **2**, **4** and for **5** + **Pt** and **6** + **Pt** was 338 K.

**Table 3** Assessment of the $N \rightleftharpoons S$ pseudorotational equilibrium in **1**–**6**

| | Compound | | | | | | | | | | | |
|---|---|---|---|---|---|---|---|---|---|---|---|---|
| | **1** | | **2** | | **3** | | **4** | | **5** | **5** + **Pt** | **6** | **6** + **Pt** |
| Protonation state | neutral | deprot. | neutral | deprot. | neutral | deprot. | neutral | deprot. | neutral | neutral | neutral | neutral |
| pH* | 6.8 | 12.5 | 6.8 | 12.1 | 6.6 | 12.1 | 6.9 | 12.2 | 6.8 | 6.8 | 6.7 | 6.8 |
| $P_N$ | −4.8 | −10.1 | −10.0 | −22.3[b] | 15.0 | 17.0[b] | 16.2 | 20.1[b] | −22.5 | −21.6 | −13.7 | −14.1 |
| $\psi_m{}^N$ | 33.2[b] | 34.1[b] | 32.3[b] | 32.8[b] | 32.5[b] | 32.9[b] | 32.5[b] | 31.6[b] | 30.5[b] | 30.5[b] | 39.3 | 39.4 |
| $P_S$ | 160.7 | 158.7 | 165.8 | 157.4 | 158.1 | 158.6 | 161.9 | 156.6 | 153.2 | 151.7 | 111.8 | 111.1 |
| $\psi_m{}^S$ | 33.2 | 34.1 | 32.2[b] | 32.9 | 32.5 | 32.9 | 32.5[b] | 31.6 | 30.5 | 30.5 | 39.3[b] | 39.4[b] |
| r.m.s. | 0.09 | 0.04 | 0.06 | 0.10 | 0.04 | 0.06 | 0.08 | 0.04 | 0.28 | 0.30 | 0.07 | 0.07 |
| $\Delta J_{max}$ | 0.19 | 0.10 | 0.14 | 0.25 | 0.06 | 0.13 | 0.23 | 0.08 | 0.52 | 0.58 | 0.17 | 0.15 |
| %$S$ (278 K) | 79.1 | 79.2 | 59.7 | 67.4 | 79.8 | 82.8 | 54.8 | 81.3 | 85.3 | 85.0 | 26.8 | 26.8 |
| %$S$ (358 K) | 74.3 | 76.9 | 61.3 | 71.0 | 71.8 | 73.2 | 55.5 | 68.8 | 77.9 | 77.8 | 35.5 | 35.3 |
| $\Delta H°$ | −2.8 | −1.5 | 0.7 | 1.8 | −4.6 | −6.0 | 0.3 | −6.7 | −5.0 | −4.9 | 4.2 | 4.1 |
| $\Delta S°$ | 0.7 | 5.9 | 5.8 | 12.4 | −5.1 | −8.4 | 2.6 | −12.3 | −3.5 | −3.4 | 6.6 | 6.2 |
| $-T\Delta S°$ (298 K) | −0.2 | −1.8 | −1.7 | −3.7 | 1.5 | 2.5 | −0.8 | 3.7 | 1.0 | 1.0 | −2.0 | −1.9 |
| $\Delta G°$ (298 K) | −3.0 | −3.3 | −1.0 | −1.9 | −3.1 | −3.5 | −0.5 | −3.0 | −4.0 | −3.9 | 2.2 | 2.2 |

[a] Pseudorotational parameters are given in degrees, root-mean-square error and $\Delta J_{max}$ are in Hz, $\Delta H°$ (±0.2), $\Delta G°$ (±0.2) and $-T\Delta S°$ (±0.5) are in kJ mol$^{-1}$, $\Delta S°$ are in J mol$^{-1}$ K$^{-1}$. [b] The pseudorotational parameter was kept fixed during the iterative optimization procedure.

is increased to 358 K. The platinum complexes **2** and **4** showed a lower preference for $\beta^t$ rotamers by 2 and 5 percentage points at 278 K in comparison with their parent nucleotides **1** and **3**, respectively. In contrast, apurinic sugar analogues **5** and **6** showed only minor conformational changes below 2 percentage points upon addition of $Pt^{2+}$ reagent, suggesting that there are no electrostatic interactions with their constituent phosphate moieties, which is also in agreement with the negligible $\Delta\delta(^{31}P)$-values (Table 1).

### Conformational equilibrium across the C4′–C5′ ($\gamma$) bond

Conformational analysis[32] of the $^3J_{4'5'}$ and $^3J_{4'5''}$ coupling constants (Table 2) has shown that $\gamma^+$ rotamers are preferred by over 59% at 278 K in **1**–**4** (Table 4). Comparison of the populations of $\gamma$ rotamers in **1** and **3** with those in **2** and **4**, respectively, showed that N7 platination exerted only a minor, if any, effect on the conformational equilibria across their C4′–C5′ bonds. Conformational analysis has also shown that $\gamma^+$ and $\gamma^t$ rotamers are highly preferred over $\gamma^-$ rotamers in apurinic analogues **5** and **6** (Table 4). As no reaction occurred between the $Pt^{2+}$ reagent and apurinic sugars **5** and **6**, no conformational changes were observed, as expected.

### Conformational equilibrium across the C3′–O3′ ($\varepsilon$) bond

The temperature-dependent $^3J_{H3'P}$, $^3J_{C4'P}$ and $^3J_{C2'P}$ coupling constants in **1**–**6** (Table 2) have been used for the evaluation of conformational equilibria across C3′–O3′ bonds (torsion angle $\varepsilon$[C4′–C3′–O3′–P]). Preliminary interpretation of the experimental coupling constants in terms of a two-state $\varepsilon^t \rightleftharpoons \varepsilon^-$ conformational equilibrium[33] resulted in large errors of up to 1.0 Hz for individual $^3J_{CP}$ coupling constants. Therefore a further attempt has been made to interpret experimental $^3J_{H3'P}$, $^3J_{C4'P}$ and $^3J_{C2'P}$ coupling constants in terms of a three-state $\varepsilon^{t,N} \rightleftharpoons \varepsilon^{t,S} \rightleftharpoons \varepsilon^{-,S}$ conformational equilibrium (Fig. 3).[34]

The least-squares optimization procedure resulted in an r.m.s. error below 0.6 Hz and a maximum discrepancy between experimental and calculated coupling constants below 0.7 Hz (Table 4). The population of $\varepsilon^{t,N}$ conformers at 278 K was 28 and 17% in **1** and **3**, respectively. Their $Pt^{2+}$ complexes **2** and **4** showed considerably higher $\varepsilon^{t,N}$ populations of 48 and 49% at 278 K, respectively. Similarly, the analysis of $^4J_{H2'P}$ coupling constants[35] in **1**–**4** showed that the population of $\varepsilon^-$ rotamers decreases (*i.e.*, $\varepsilon^t$ increases) upon platination of the nucleobase. The higher preference for $\varepsilon^t$ rotamers in $Pt^{2+}$ complexes **2** and **4** is correlated with the higher preference for *N*-type pseudo-

View Article Online

**Table 4** Conformational equilibria across $\beta$, $\gamma$ and $\varepsilon$ torsion angles in **1**–**6** at two limiting temperatures

| Compd. | $T$(K) | $\beta$ torsion [a] | $\gamma$ torsion [b] | | | $\varepsilon$ torsion [c] | | | | | | | |
|---|---|---|---|---|---|---|---|---|---|---|---|---|---|
| | | $\%\beta^{t}$ | $\%\gamma^{+}$ | $\%\gamma^{t}$ | $\%\gamma^{-}$ | $\varepsilon^{t,N}$ (°) | $\varepsilon^{t,S}$ (°) | $\varepsilon^{-,S}$ (°) | $\%\varepsilon^{t,N}$ | $\%\varepsilon^{t,S}$ | $\%\varepsilon^{-,S}$ | r.m.s. (Hz) | $\Delta J^{max}$ (Hz) |
| **1** | 278 | 81 | 61 | 10 | 29 | 221 | 190 | 267 | 28 | 35 | 37 | 0.076 | <0.1 |
| | 358 | 77 | 50 | 35 | 15 | | | | 37 | 32 | 31 | | |
| **2** | 278 | 79 | 59 | 27 | 14 | 214 | 192 | 263 | 48 | 26 | 27 | 0.331 | 0.4 |
| | 358 | 75 | 50 | 34 | 17 | | | | 31 | 32 | 37 | | |
| **3** | 278 | 82 | 73 | 18 | 10 | 211 | 192 | 261 | 17 | 11 | 72 | 0.587 | 0.7 |
| | 358 | 76 | 62 | 29 | 9 | | | | 27 | 16 | 57 | | |
| **4** | 278 | 77 | 73 | 21 | 6 | 211 | 192 | 266 | 49 | 14 | 36 | 0.107 | 0.1 |
| | 358 | 76 | 59 | 32 | 9 | | | | 53 | 9 | 38 | | |
| **5** | 278 | 75 | 44 | 38 | 18 | 212 | 197 | 260 | 17 | 43 | 40 | 0.079 | 0.1 |
| | 358 | 71 | 39 | 41 | 20 | | | | 0 | 56 | 44 | | |
| **5** + **Pt** | 278 | 75 | 44 | 37 | 20 | 213 | 198 | 266 | 15 | 46 | 40 | 0.038 | <0.1 |
| | 358 | 70 | 38 | 41 | 21 | | | | 21 | 41 | 36 | | |
| **6** | 278 | 77 | 61 | 35 | 4 | 212 | 192 | 266 | 70 | 0 | 30 | 0.218 | 0.3 |
| | 358 | 73 | 53 | 40 | 6 | | | | 51 | 13 | 37 | | |
| **6** + **Pt** | 278 | 76 | 60 | 36 | 4 | 210 | 191 | 267 | 67 | 0 | 33 | 0.104 | 0.1 |
| | 358 | 72 | 51 | 41 | 7 | | | | 57 | 9 | 34 | | |

[a] The populations of $\beta^{t}$ conformers (±3%) have been calculated independently from $^{3}J_{CP}$ and $^{3}J_{HP}$ acquired in the temperature range from 278 to 358 K in 20 K steps and their average values are reported. For **2**, **4**, **5** + **Pt** and **6** + **Pt** the populations of $\beta^{t}$ conformers at 358 K have been calculated from $^{3}J_{HP}$ only. [b] The populations of $\gamma$ conformers (±3%) have been calculated from $^{3}J_{4'5'}$ and $^{3}J_{4'5''}$. [c] The highest temperature for the collection of $^{13}$C NMR data for complexes **2** and **4** and for **5** + **Pt** and **6** + **Pt** was 338 K, which is the highest temperature where the populations of $\varepsilon^{t,N}$, $\varepsilon^{t,S}$ and $\varepsilon^{-,S}$ conformers (±5%) are reported.

Published on 01 January 1999. Downloaded on 22/10/2014 10:06:02.

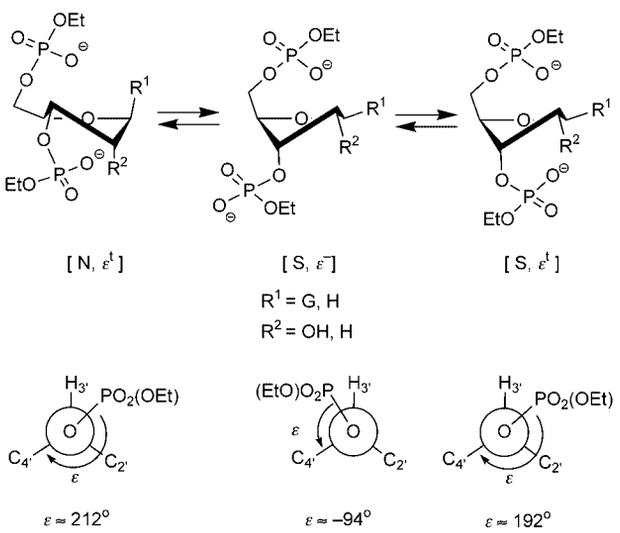


**Fig. 3** A hypothetical three-state conformational equilibrium across C3′–O3′ bonds in **1**–**6**.

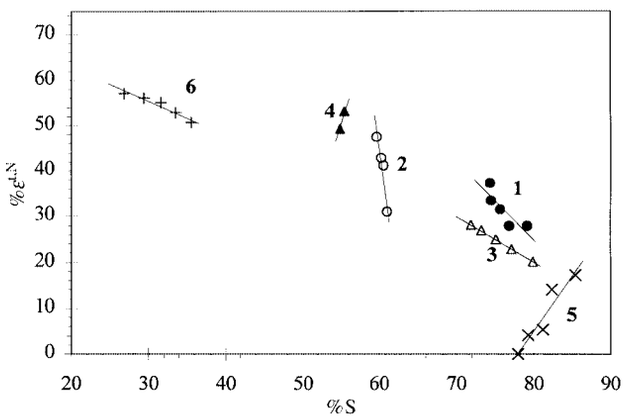


**Fig. 4** Correlation plots between the populations of $\varepsilon^{t,N}$ conformers and the populations of *S*-type pseudorotamers in **1**–**6**. The least-squares-fitted straight lines were calculated from the mole fractions of *S*-type pseudorotamers obtained by the PSEUROT analysis of temperature-dependent $^{3}J_{HH}$ coupling constants, and the respective mole fractions of $\varepsilon^{t,N}$ conformers obtained from the analysis of $^{3}J_{HP}$ and $^{3}J_{CP}$ coupling constants. Their Pearson's correlation coefficients are −0.859 for **1**, −0.965 for **2**, 1.000 for **3** and **4**, 0.951 for **5** and −0.966 for **6**. Note that for **1**, **2**, **5** and **6** five experimental data points were available from the temperature-dependent coupling constants in the range from 278 to 358 K in 20 K steps. In the case of platinum complexes **2** and **4** four sets of populations were determined in the temperature range from 278 to 338 K in 20 K steps. The populations of *S*-type pseudorotamers in **4** change by <1 percentage point from 278 to 338 K in 20 K steps which results in the overlap of some data points.

rotamers.[33] Correlations of populations of $\varepsilon^{t,N}$ and *S*-type conformers in **1**–**6** are shown in Fig. 4. The least-squares fitting procedure afforded straight lines which indicate that as the population of *S*-type pseudorotamers decreases with increasing temperature in **1** and **3**, the population of $\varepsilon^{t,N}$ conformers increases.

### Conformational equilibria across $CH_2$–O ($\varepsilon^{-1}$) and O–$CH_2$ ($\beta^{+1}$) bonds

The structural make-up of **1**–**6** gives insight into the tunability as well as the energetic transmission characteristics of the $N \rightleftharpoons S$ pseudorotational equilibrium to drive the rotamer distribution along the phosphate backbone as a result of formation of the new Pt–N7 bond in **2** and **4** compared with the parent nucleotides **1** and **3** and abasic bis-phosphates **5** and **6**. We argued that this should in turn show how the dynamics of the conformational cooperativity in the immediate micromilieu changes and is transmitted as a result of ligand binding. There is, however, no *J*-coupling that would give insight into $\alpha$ and $\zeta$ torsions (Chart 1) which are the closest to $\varepsilon$, where a linear correlation between increased population of *N*-type pseudorotamers and $\varepsilon^{t,N}$ conformers has been observed (Fig. 4). It is interesting to note that methylene protons of 3′-ethyl phosphodiester groups in 2′-deoxynucleotide **1** and its platinum complex **2** are isochronous at all temperatures from 278 to 358 K, which suggests their unperturbed rotation. The methylene protons of 3′-ethyl phosphodiester groups in **3** and **4** were non-isochronous ($\Delta\delta = 10$ and 7 Hz at 278 K and $\Delta\delta = 5$ and 4 Hz at 358 K, respectively) which implies the specific role of 2′-OH interacting with the vicinal ethyl phosphate. The conformational equilibria across $\beta^{+1}$ torsion angles in **1**–**6** were evaluated on the basis of both temperature-dependent $^{3}J_{CH3P}$ and the sum of $^{3}J_{CH2P}$ coupling constants.[29–31] The population of $\beta^{+1}$-*trans* rotamers was ≈57% at 278 K and decreased by 4 to 5 percentage points upon an increase of temperature to 358 K in **1**–**4**. On

View Article Online

Published on 01 January 1999. Downloaded on 22/10/2014 10:06:02.

the other hand, the platination of **1** and **3** caused negligible conformational changes across their $\beta^{+1}$ torsion angles. The spectral overlap of methylene resonances of 3′-ethyl phosphodiester groups in **5** and **6** prevented determination of their $^1$H NMR chemical shifts and extraction of individual $^3J_{CH2P}$ coupling constants. The analysis of $^3J_{CH3P}$ coupling constants in 3′-ethyl phosphodiester groups in **5** and **6** showed that the preference for $\beta^{+1}$-*trans* rotamers drops by ≈4 percentage points with the increase of temperature from 278 to 358 K.

The methylene protons of 5′-ethyl phosphodiester groups in **2** are non-isochronous ($\Delta\delta$ = 16 Hz at 278 K and 9 Hz at 358 K), whereas they are isochronous in **1**. In the case of *ribo* counterparts **3** and **4** we have observed the non-equivalence of the methylene protons of 5′-ethyl phosphodiester groups up to 338 K in **3** ($\Delta\delta$ = 11 Hz at 278 K and $\Delta\delta$ = 5 Hz at 318 K) and up to 358 K in **4** ($\Delta\delta$ = 10 Hz at 278 K and 5 Hz at 358 K). The appearance of non-isochronous methylene protons of 5′-ethyl phosphodiester groups in **2** and **4** in comparison to **1** and **3** suggests some electrostatic interactions between platinum and phosphate oxygen atoms. Note that $\Delta\delta$-values for $^{31}$P upon platination of **1** and **3** were below 0.06 ppm (Table 1) and did not provide any conclusive evidence about such chelative interactions. The conformational equilibria across $\varepsilon^{-1}$ torsion angles in **1**–**6** were evaluated on the basis of both temperature-dependent $^3J_{CH3P}$ and the sum of $^3J_{CH2P}$ coupling constants of the 5′-ethyl hydrogen phosphate moiety. The population of $\varepsilon^{-1}$-*trans* rotamers was ≈57% at 278 K and decreased by 1 to 5 percentage points upon an increase of temperature to 358 K. The platination of **1** and **3** caused negligible conformational changes across $\varepsilon^{-1}$ torsion angle. In the case of abasic bisphosphate analogues **5** and **6**, the heavy spectral overlap prevented the extraction of $\Delta\delta$-values of their methylene protons and $^3J_{CH2P}$ coupling constants. The analysis of $^3J_{CH3P}$ coupling constants in 5′-ethyl phosphodiester groups in **5** and **6** showed that the preference for $\varepsilon^{-1}$-*trans* rotamers drops by ≈6 percentage points with an increase of temperature from 278 to 358 K. The addition of platination reagent to **5** and **6** caused negligible change in the population of $\varepsilon^{-1}$ rotamers.

### Electron delocalization caused by $Pt^{2+}$ binding to N7 steers sugar-phosphate conformation

It is known that the binding of cisplatin to DNA is followed by structural distortions leading to duplex bending and unwinding that are recognized by HMG proteins.[36] Our data clearly show that there are important electronic and thermodynamic consequences of the formation of bifunctional complexes with cisplatin. Two simple model mononucleotides, 2′-deoxyguanosine 3′,5′-bis(ethyl hydrogen phosphate) **1** and its *ribo* analogue **3**, were prepared in order to understand how the local microstructure changes as a consequence of $Pt^{2+}$ binding to the guanine moiety in a polynucleotide. Comparative analysis of multinuclear NMR chemical-shift data of abasic bisphosphodiesters **5** and **6** clearly showed the absence of any interactions of $Pt^{2+}$ with anionic phosphates. The $N \rightleftharpoons S$ pseudorotational equilibrium in **2** and **4** has been shifted towards *N*-type conformers by 17 and 21 percentage points at 298 K, respectively. The increase in the population of *N*-type conformers caused by the formation of Pt–N7 bonds in **2** and **4** promotes $n_{O4'} \rightarrow \sigma^*_{C1'\text{-}N9}$ orbital interactions due to the re-distribution of π-electron density and thus strengthens the anomeric effect of guanine in both 2′-deoxy and *ribo* nucleotides. The additional stabilization of *N*-type conformers in $Pt^{2+}$ complexes of the ribonucleotides is due to the tuning of the *gauche* effect of [N9–C1′–C2′–O2′] fragment which is absent in 2′-deoxy-*ribo* counterparts.

The platination of N7 makes N1–H more acidic, and thus N1 deprotonations in **2** and **4** are favoured by $\Delta pK_a$ of 0.7 and 0.9 units in comparison with parent nucleotides **1** and **3**, respectively, which might somewhat facilitate the base-pairing of $Pt^{2+}$–guanine complex with a cytosine moiety more strongly through hydrogen bonding or binding to any other basic ligand, compared with the free guanine nucleotide moieties. The $N \rightleftharpoons S$ pseudorotational equilibrium in **1**–**4** showed classical sigmoidal dependence as a function of pH with $pK_a$-values at the inflection points. The population of *S*-type conformers at 298 K increased upon N1 deprotonation from 76 to 79% in **1**, from 57 to 67% in **2**, from 76 to 80% in **3** and from 51 to 73% in **4**, which showed that the thermodynamics of N1 deprotonation in guanine nucleosides is transmitted through the tunable anomeric effect to drive the $N \rightleftharpoons S$ equilibrium towards *S*-type pseudorotamers. The $Pt^{2+}$-complex bound to N7 was found to promote the re-distribution of the π-electronic density from anionic deprotonated N1, which results in the larger increase in the population of *S*-type conformers by 10 percentage points in **2** and by 22 percentage points in **4** in comparison with parent nucleotides **1** and **3** respectively.

The formation of the Pt–N7 bond simultaneously causes a shift of the *syn* $\rightleftharpoons$ *anti* equilibrium towards *anti* by 43 and 63 percentage points in bifunctional complexes **2** and **4**, and an increase in the population of $\varepsilon^{t,N}$ conformers by 20 and 32 percentage points at 278 K, respectively. Only minor conformational re-distributions along $\beta$, $\gamma$, $\beta^{+1}$ and $\varepsilon^{-1}$ torsion angles have been observed which suggests weak conformational co-operativity between the shift in the $N \rightleftharpoons S$ pseudorotational equilibrium towards *N*-type conformers and the conformational changes across phosphate torsion angles other than $\varepsilon$. The apurinic 3′,5′-bis(ethyl hydrogen phosphate) sugars **5** and **6** showed no interaction with $Pt^{2+}$ and therefore no conformational changes.

## Experimental

### General procedures in synthesis

Compounds **7** and **9** were synthesized using standard procedures[37,38] starting from 2′-deoxyguanosine and guanosine, respectively (Scheme 1). Protected nucleosides were converted into 3′,5′-bis(phosphotriesters) **8** and **10** by treatment with (2-cyanoethoxy)(*N*,*N*-diisopropylamino)(ethoxy)phosphine[39] in DMF–MeCN solution at r.t. under nitrogen atmosphere in the presence of tetrazole followed by oxidation of the intermediary phosphite triesters by aq. iodine solution with yields of 60 and 91%, respectively. Deprotections of these compounds were carried out using aq. ammonia and 80% aq. acetic acid for removing of MDMP (3-methoxy-1,5-dimethoxycarbonylpent-3-yl) group of **11** to give fully deprotected 3′,5′-bis(phosphodiesters) **1** (73%) and **3** (57%).

1-Deoxyribofuranose derivative **15** was obtained from 1,2,3,5-tetra-*O*-acetyl-β-D-ribofuranose *via* conversion into the 1-phenylthio derivative using boron trifluoride–diethyl ether as catalyst (70%) followed by reduction by a modified literature procedure (80%),[15] deprotection using methanolic ammonia (96%) and protection as the 3,5-*O*-(1,1,3,3-tetraisopropyldisiloxane-1,3-diyl) derivative (75%).[40] Part of this compound was converted to **15** according to the literature procedure (60%),[41] whereas the other part was reduced (60%)[42] and converted[15] to the 1,2-dideoxy derivative **12** (60%). C5 of deoxyribose derivatives **12** and **15** was protected since 3-phosphotriesters **14** and **17** were to be used as intermediates for the synthesis of 3,5-bis(phosphodiesters) having an *O*-methyl hydrogen phosphate group at the C5 position. 3,5-Bis(phosphotriesters) **18** (90%) and **19** (70%) were prepared by phosphorylation of the 3-hydroxy group by (2-cyanoethoxy)-(*N*,*N*-diisopropylamino)(ethoxy)phosphine in DMF–MeCN solution at r.t. under nitrogen atmosphere in the presence of tetrazole followed by oxidation by aq. iodine solution to give compounds **13** (80%) and **16** (83%), followed by removal of 5-*O*-protection by 80% acetic acid (η 84% for compound **14**) or by 0.1 M trichloroacetic acid (η 83% for compound **17**) and

View Article Online

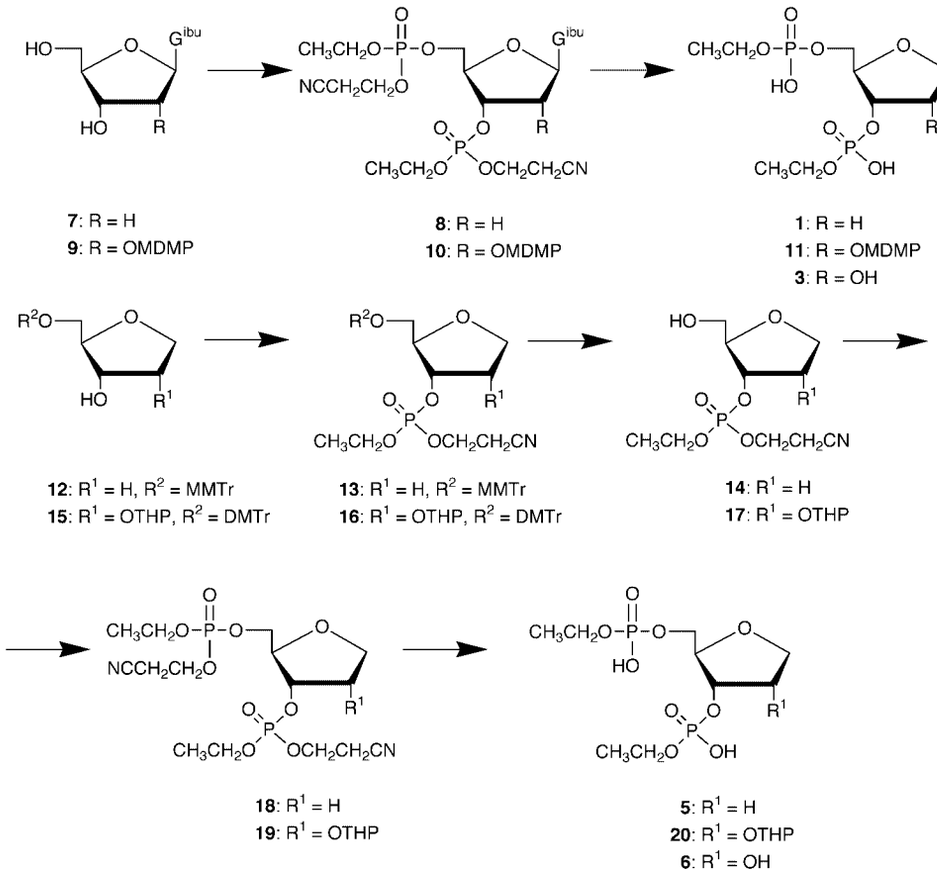


**Scheme 1** Synthesis of **1**, **3**, **5** and **6**.

phosphorylation of 5-OH by the procedure described above. 3,5-Bis(phosphotriesters) of deoxyribofuranose, derivatives **18** and **19**, were converted into appropriate bis(phosphodiesters) **5** (86%) and **20** by treatment with aq. ammonia. The tetrahydropyranyl group of **20** was cleaved by 10% aq. acetic acid (pH > 3)[43] to afford compound **6** (57%). All 3,5-bis(phosphodiesters) were converted into the dirodium salt by passage through Dowex 50 WX8 resin ($Na^+$-form).

### Preparation of $Pt^{2+}$ complexes

A 10 mM solution of the activated form of cisplatin, *cis*-$[Pt(ND_3)_2(D_2O)_2]^{2+}$, was prepared by suspending *cis*-$[Pt(NH_3)_2Cl_2]$ in $D_2O$ (99.9% D) containing two equivalents of $AgNO_3$. The suspension was stirred vigorously overnight. After removal of AgCl, the solution was stored in a closed vial at 5 °C in the dark (pH* ≈ 3). Fresh solutions of *cis*-$[Pt(ND_3)_2(D_2O)_2]^{2+}$ ($\delta_{Pt} = -1613$ ppm) were prepared no more than one day before the experiment. Two molar equivalents of **1**, **3**, **5** and **6** were dissolved in a 10 mM solution of *cis*-$[Pt(ND_3)_2(D_2O)_2]^{2+}$ and the reaction mixture was stirred at 25 °C for 20 h to form the bifunctional complex.

### NMR Measurements

$^1H$, $^{13}C$, $^{31}P$ and $^{15}N$ NMR spectra were acquired at 600.07, 150.91, 242.91 and 60.82 MHz, respectively, on a Varian Unity Inova 600 NMR spectrometer at the National NMR Center of Slovenia. $^{195}Pt$ spectra were recorded at 64.325 MHz on a Varian Unity Plus 300. Sample concentration was 20 mM in $D_2O$ (99.9% D) at a neutral pH* of 6.8 ± 0.3. The pH* values were measured with a combined glass electrode calibrated with standard buffers with pH of 4, 7 and 10 in $H_2O$ and were not corrected for the deuterium isotope effect. 3-(Trimethylsilyl) propionic acid was used as internal standard for $^1H$ and $^{13}C$ NMR ($\delta = 0$ ppm) spectra, MeCN ($\delta = -135.8$ ppm) as external reference for $^{15}N$ NMR spectra, 85% aq. $H_3PO_4$ ($\delta = 0$ ppm) as external reference for $^{31}P$ NMR spectra and $Na_2PtCl_6$ as external reference for $^{195}Pt$ spectra ($\delta = 0$ ppm). The errors in chemical-shift determinations were: ±0.001 ppm for $^1H$, ±0.01 ppm for $^{13}C$ and $^{31}P$, ±0.5 ppm for $^{15}N$, and ±1 ppm for $^{195}Pt$. The sample temperature was varied from 275 K to 358 K in 20 K steps and controlled to approximately ±0.5 K. The error in $^3J_{HH}$ was 0.1 Hz as estimated from a comparison of the experimental and simulated spectra.

### Conformational analysis

Conformational analysis of the sugar moiety has been performed by the computer program PSEUROT[27] with the use of λ electronegativities[44] for the substituents along H–C–C–H fragments. In the optimization procedure the geometries and populations of both *N*- and *S*-type pseudorotamers were varied to obtain the best fit between the experimental and the calculated coupling constants. Our optimization procedure started with the following input values: $P_N = 18°$, $\Psi_m{}^N = 36°$, $P_S = 156°$ and $\Psi_m{}^S = 36°$. In the case of **1**, **3**, **5** and **6** the puckering amplitude of the minor conformer was kept frozen during the individual iterative least-squares optimization, whereas in the case of **2** and **4** the puckering amplitudes of both conformers ($\Psi_m{}^N$ and $\Psi_m{}^S$) were constrained while all other parameters were freely optimized. The following ranges of *P* and $\Psi_m$ were found to fit with experimental $^3J_{HH}$ data within root-mean-square error <0.3 Hz and $\Delta J_{max}$ <0.5 Hz: $-20° < P_N < 20°$, $33° < \Psi_m{}^N < 34°$, $157° < P_S < 165°$, $33° < \Psi_m{}^S < 34°$ for **1**, $-11° < P_N < -7°$, $29° < \Psi_m{}^N < 35°$, $163° < P_S < 176°$, $29° < \Psi_m{}^S < 35°$ for **2**, $-40° < P_N < 50°$, $33° < \Psi_m{}^N < 40°$, $140° < P_S < 174°$, $33° < \Psi_m{}^S < 40°$ for **3**, $16° < P_N < 48°$, $32° < \Psi_m{}^N < 38°$, $160° < P_S < 198°$, $32° < \psi_m{}^S < 38°$ for **4**, $-25° < P_N < -5°$, $30° < \Psi_m{}^N < 31°$, $154° < P_S < 156°$, $31° < \Psi_m{}^S < 32°$ for **5**, $-20° < P_N < -5°$, $39° < \Psi_m{}^N < 41°$, $102° < P_S < 123°$, $39° < \Psi_m{}^S < 41°$ for **6**.



Published on 01 January 1999. Downloaded on 22/10/2014 10:06:02.

View Article Online

The interpretation of the experimental $^3J_{C4'P}$, $^3J_{C2'P}$ and $^3J_{H3'P}$ coupling constants has been performed with the assumption of a three-state $\varepsilon^{t,N} \rightleftharpoons \varepsilon^{t,S} \rightleftharpoons \varepsilon^{-,S}$ conformational equilibrium. The three-parameter Karplus equations [34] for $^3J_{CP} = 9.1\cos^2\Phi - 1.9\cos\Phi + 0.8$ and $^3J_{HP} = 15.3\cos^2\Phi - 6.2\cos\Phi + 1.5$ have been used in the calculation of $^3J_{CP}$ and $^3J_{HP}$ coupling constants from the $\varepsilon$ torsion angles in the hypothetical $\varepsilon^{t,S}$, $\varepsilon^{-,S}$ and $\varepsilon^{t,N}$ conformers and their respective populations, which were iterated to find the best fit with the experimental temperature-dependent $^3J_{C4'P}$, $^3J_{C2'P}$ and $^3J_{H3'P}$ coupling constants.

### Acid–base properties

The p$K_a$-values of **1**–**4** (Fig. 2A) were calculated from the sigmoidal curves which were the best iterative least-squares fits (r.m.s. error < 0.003 ppm) of the pH*-dependent experimental $^1$H NMR chemical shifts according to the Henderson–Hesselbach equation (1):

$$\mathrm{pH^*} = \mathrm{p}K_a + \log\frac{[\mathrm{A}]}{[\mathrm{AH}]} = \mathrm{p}K_a + \log\frac{1-\alpha}{\alpha} \qquad (1)$$

We have additionally constructed Hill plots of pH* as a function of the logarithm of the ratio of the protonated and deprotonated species. The Pearson's correlation coefficients ($R$) of the linear regression lines in Hill plots are above 0.994 for **1**–**4**. The slopes are close to 1, which is the characteristic indication for the protonation involving a single protonation site. The populations of *S*-type pseudorotamers and $\Delta G^\circ$ as a function of pH* (Fig. 2B and 2C) were analyzed in a similar way.

## Acknowledgements

We thank the Ministry of Science and Technology of Republic of Slovenia (Grant No. Z1-8609-0104), and the Swedish Natural Science Research Council (NFR), the Swedish Board for Technical Development (NUTEK) and the Swedish Engineering Research Council (TFR) for generous financial support.

## References

1 M. J. Bloemink and J. Reedijk, in *Metal Ions in Biological Systems*, ed. A. Sigel and H. Sigel, Marcel Dekker Inc., New York, 1996, vol. 32, pp. 641–685.
2 D. Kiser, F. P. Intini, Y. Xu, G. Natile and L. G. Marzilli, *Inorg. Chem.*, 1994, **33**, 4149.
3 S. K. Miller and L. G. Marzilli, *Inorg. Chem.*, 1985, **24**, 2421.
4 S. O. Ano, F. P. Intini, G. Natile and L. G. Marzilli, *J. Am. Chem. Soc.*, 1998, **120**, 12017.
5 S. O. Ano, F. P. Intini, G. Natile and L. G. Marzilli, *J. Am. Chem. Soc.*, 1997, **119**, 8570.
6 Z. J. Guo, Y. Chen, E. Zang and P. J. Sadler, *J. Chem. Soc., Dalton Trans.*, 1997, 4107.
7 J. M. Teuben, S. S. G. E. van Boom and J. Reedijk, *J. Chem. Soc., Dalton Trans.*, 1997, 3979.
8 M. J. Bloemink, E. L. M. Lempers and J. Reedijk, *Inorg. Chim. Acta*, 1990, **176**, 317.
9 F. J. Dijt, G. W. Canters, J. H. J. den Hartog, A. T. M. Marcelis and J. Reedijk, *J. Am. Chem. Soc.*, 1984, **106**, 3644.
10 B. Song, G. Oswald, J. Zhao, B. Lippert and H. Sigel, *Inorg. Chem.*, 1998, **37**, 4857.
11 H. Sigel, B. Song, G. Oswald and B. Lippert, *Chem. Eur. J.*, 1998, **4**, 1053.
12 H. P. M. de Leeuw, C. A. G. Haasnoot and C. Altona, *Isr. J. Chem.*, 1980, **20**, 108.
13 C. Altona and M. Sundaralingam, *J. Am. Chem. Soc.*, 1972, **94**, 8205.
14 C. Altona and M. Sundaralingam, *J. Am. Chem. Soc.*, 1973, **95**, 2333.
15 J. Plavec, W. Tong and J. Chattopadhyaya, *J. Am. Chem. Soc.*, 1993, **115**, 9734.
16 J. Plavec, C. Thibaudeau and J. Chattopadhyaya, *Pure Appl. Chem.*, 1996, **68**, 2137.
17 C. Thibaudeau, J. Plavec and J. Chattopadhyaya, *J. Org. Chem.*, 1996, **61**, 266.
18 M. Polak and J. Plavec, *Nucleosides, Nucleotides*, 1998, **17**, 2011.
19 M. Polak and J. Plavec, *Eur. J. Inorg. Chem.*, 1999, 547.
20 H. Huang, L. Zhu, B. R. Reid, G. P. Drobny and P. B. Hopkins, *Science*, 1995, **270**, 1842.
21 J. Arpalahti, M. Mikola and S. Mauristo, *Inorg. Chem.*, 1993, **32**, 3327.
22 M. Mikola, K. D. Klika, A. Hakala and J. Arpalahti, *Inorg. Chem.*, 1999, **38**, 571.
23 M. D. Reily and L. G. Marzilli, *J. Am. Chem. Soc.*, 1986, **108**, 8299.
24 J. Kozelka and G. Barre, *Chem. Eur. J.*, 1997, **3**, 1405.
25 R. B. Martin, *Chem. Rev.*, 1996, **96**, 3043.
26 F. A. A. M. de Leeuw and C. Altona, *J. Comput. Chem.*, 1983, **4**, 428.
27 C. Haasnoot, F. A. A. M. de Leeuw, D. Huckriede, J. van Wijk and C. Altona, PSEUROT – A program for the conformational analysis of five membered rings, Leiden, Netherlands, 1993.
28 H. Rosemeyer, G. Toth, B. Golankiewicz, Z. Kazimierczuk, W. Bourgeois, U. Kretschmer, H.-P. Muth and F. Seela, *J. Org. Chem.*, 1990, **55**, 5784.
29 P. P. Lankhorst, C. A. G. Haasnoot, C. Erkelens and C. Altona, *J. Biomol. Struct. Dyn.*, 1984, **1**, 1387.
30 M. M. W. Mooren, S. S. Wijmenga, G. A. van der Marel, J. H. van Boom and C. W. Hilbers, *Nucleic Acids Res.*, 1994, **22**, 2658.
31 J. Plavec and J. Chattopadhyaya, *Tetrahedron Lett.*, 1995, **36**, 1949.
32 C. A. G. Haasnoot, F. A. A. M. de Leeuw, H. P. M. de Leeuw and C. Altona, *Recl. Trav. Chim. Pays-Bas*, 1979, **98**, 576.
33 J. Plavec, C. Thibaudeau, G. Viswanadham, A. Sandström and J. Chattopadhyaya, *Tetrahedron*, 1995, **51**, 11775.
34 P. P. Lankhorst, C. A. G. Haasnoot, C. Erkelens, H. P. Westerink, G. A. van der Marel, J. H. van Boom and C. Altona, *Nucleic Acids Res.*, 1985, **13**, 927.
35 M. J. J. Blommers, D. Nanz and O. Zerbe, *J. Biomol. NMR*, 1994, **4**, 595.
36 A. Gelasco and S. J. Lippard, *Biochemistry*, 1998, **37**, 9230.
37 G. S. Ti, B. L. Gaffney and R. A. Jones, *J. Am. Chem. Soc.*, 1982, **104**, 1316.
38 A. Sandström, M. Kwiatkowski and J. Chattopadhyaya, *Acta Chem. Scand., Sect. B*, 1985, **39**, 273.
39 C. Sund, P. Agback, L. H. Koole, A. Sandström and J. Chattopadhyaya, *Tetrahedron*, 1992, **48**, 695.
40 W. T. Markiewicz, *J. Chem. Res. (S)*, 1979, 24.
41 B. E. Griffin, M. Jarman and C. B. Reese, *Tetrahedron*, 1968, **24**, 639.
42 M. J. Robins, J. S. Wilson and F. Hansske, *J. Am. Chem. Soc.*, 1983, **105**, 4059.
43 M. A. Morgan, S. A. Kazakov and S. M. Hecht, *Nucleic Acids Res.*, 1995, **23**, 3949.
44 C. Altona, R. Francke, R. de Haan, J. H. Ippel, G. J. Daalmans, A. J. A. Westra Hoekzema and J. van Wijk, *Magn. Reson. Chem.*, 1994, **32**, 670.

*Paper 9/02330E*

Published on 01 January 1999. Downloaded on 22/10/2014 10:06:02.